Research Inventy: International Journal of Engineering And Science
Vol.13, Issue 6 (June 2023), PP 01-13
Issn (e): 2278-4721, Issn (p):2319-6483, www.researchinventy.com

Treatment of Hydrophobic Polyaromatic Hydrocarbons (PAHs) using Graphene oxide/Strontium carbonate ($GO/SrCO_3$) Nanocomposite via Photocatalytic Degradation and the Evaluation of Experimental Results with Microtox and *Daphnia magna* Acute Toxicity Assays

Rukiye Öztekin [a], Delia Teresa Sponza [a, *]

[a] *Dokuz Eylül University, Engineering Faculty, Department of Environmental Engineering, Tınaztepe Campus, 35160 Buca/Izmir, Turkey, Tel. +90 232 301 7119; Fax: + 90 232 453 11 43; E-mails: delya.sponza@deu.edu.tr (Prof. Dr. Delia Teresa Sponza); rukiyeoztekin@gmail.com (Post-Dr. Rukiye Öztekin).*

** Corresponding Author: Prof. Dr. Delia Teresa Sponza, Dokuz Eylül University, Engineering Faculty, Department of Environmental Engineering, Tınaztepe Campus, 35160 Buca/Izmir, Turkey*

ABSTRACT

The effects of increasing sun light irradiaiton time (60 min, 120 min, 180 and 240 min), increasing photocatalytic power (40 W, 80 W and 120 W), increasing graphene oxide/strontium carbonate ($GO/SrCO_3$) nanocomposites (NCs) concentrations (1 mg/l, 5 and 10 mg/l) on the destructions of four hydrophobic polycyclic aromatic hydrocarbons (PAHs) in a real petrochemical industry wastewater (PCI ww) in Izmir (Turkey) were investigated. The yields in more hydrophobic PAHs with high benzene rings [benzo[a]pyrene (BaP) and benzo[k]fluoranthene (BkF)] were as high as the less hydrophobic PAHs with lower benzene rings [acenaphthylene (ACL) and carbazole (CRB)] at pH=7.0, at 22°C after 240 min sun light irradiation time. The characteristics of the synthesized nanoparticles (NPs) were assessed using X-Ray Difraction (XRD), Field Emission Scanning Electron Microscopy (FESEM), Energy Dispersive X-Ray (EDX) and Fourier Transform Infrared Spectroscopy (FTIR) analyses, respectively. The acute toxicity assays were operated with Microtox (Aliivibrio fischeri or Vibrio fischeri) and Daphnia magna acute toxicity tests. Cost analysis was evaluated for hydrophobic PAHs removal with $GO/SrCO_3$ NCs by photocatalytic degradation (PCD) process in PCI ww. ANOVA statistical analysis was used for all experimental samples. Maximum 97%ACL, 98%CRB, 98%BaP and 99%BkF PAHs removals was detected at 10 mg/l $GO/SrCO_3$ NCs, at 100 mW/cm^2 sun light intensity, at 120 W, at 240 min, at pH=7.0 and at 22°C, respectively. The maximum 83%ACL, 84%CRB, 87%BaP and 89%BkF hydrophobic PAHs removals were indicated after 240 min sun light irradiation time, at 100 mW/cm^2, at 100 W, at pH=7.0 and at 22°C, respectively. The maximum 87%ACL, 90%CRB, 92%BaP and 94%BkF hydrophobic PAHs removals were indicated at 120 W photocatalytic power, at 100 mW/cm^2, after 240 min, at pH=7.0 and at 22°C, respectively. The maximum 98%ACL, 98%CRB, 98%BaP and 99%BkF hydrophobic PAHs removals were found at 10 mg/l $GO/SrCO_3$ NCs concentration at 100 mW/cm^2, at 120 W, after 240 min, at a pHof 7.0 and at 22°C, respectively. 96.47% maximum Microtox acute toxicity removals was found in $GO/SrCO_3$ NCs=10 mg/l after 180 min and at 60°C. 92.38% maximum Daphnia magna acute toxicity removal was obtained in $GO/SrCO_3$ NCs=10 mg/l after 180 min and at 60°C. Finally, $GO/SrCO_3$ NCs holds the potential to serve as a highly effective and robust photocatalyst for energy-effective photodegradation of PAHs (and potentially other persistent organic pollutants) in complex water matrices, and the multiplicative model is a useful tool for predicting the photocatalytic performances under several experimental conditions.

Keywords: *Acute toxicity; ANOVA statistical analysis; Daphnia magna; Energy Dispersive X-Ray (EDX); Field Emission Scanning Electron Microscopy (FESEM); Fourier Transform Infrared Spectroscopy (FTIR); Graphene oxide/strontium carbonate ($GO/SrCO_3$) nanocomposite; Microtox (Aliivibrio fischeri); Nanoparticles; Petrochemical industry wastewater; Photocatalytic degradation; Polycyclic aromatic hydrocarbons (PAHs); X-Ray Difraction (XRD).*

Date of Submission: 22-05-2023 Date of Acceptance: 03-06-2023

I. INTRODUCTION

PAHs are an important class of persistent organic pollutants (POPs), and have been ubiquitously found in the environment (Fu et al., 2011a). Besides the natural sources, PAHs are often from anthropogenic sources such as incomplete combustion of fossil fuels, and accidental spillages of crude and refined oils (Fu et al., 2014; Gong et al., 2015). Due to their persistence and potential harmful impact on the ecosystem and human health, PAHs have been classified as priority pollutants by the United States Environmental Protection Agency (USEPA) (Fu et al., 2011b).

Wastewater treatment plants, especially those serving industrial areas, consistently receive complex mixtures containing a wide variety of organic pollutants. Groups of compounds present in the petrochemical industries include PAHs, which are listed as US-EPA and EU priority pollutants, and concentrations of these pollutants therefore need to be controlled in treated ww effluents (Banjoo and Nelson, 2005). PAHs are ubiquitous environmental pollutants with mutagenic properties, which have not been included in the Turkish guidelines for treated waste monitoring programs (Sponza and Oztekin, 2010). Several hydroxy-PAHs such as hydroxylated derivatives of BaP and Chrysene (CHR) have been shown to possess estrogenic activity and cause damage to DNA leading to cancer and possibly other effects (Quesada-Peñate et al., 2009; Sponza and Oztekin, 2010). As a consequence of their strongly hydrophobic properties and their resistance to biodegradation, PAHs are not always quantitatively removed from ww by activated sludge treatments, which very efficiently relocate them into treated effluents.

Graphene is a flat monolayer of carbon atoms tightly packed into a two-dimensional honeycomb lattice. In recent years, graphene has attracted a great deal of attentions for its potential applications in many fields, such as nano-electronics, fuel-cell technology, supercapacitors, and catalysts (Qu et al., 2010; Liang et al. 2011). Graphene oxide (GO) is one of the most important precursors of graphene, and thus, they share similar sheet structures and properties such as high stability and semiconducting characteristics (Guo et al. 2011; Zeng et al., 2012). GO can enhance the light absorption via expanding the photoresponsive range to visible light and suppress the charge recombination by serving as a photo-generated electron transmitter, when coupled with TiO_2 (Zeng et al. 2012). To further enhance the conductivity and reduce the bandgap, noble metals (e.g., gold, palladium and platinum) are often incorporated to the GO-TiO_2 NCs by surface deposition (Zeng et al. 2012; Stengl et al., 2013).

Compared with noble metals, strontium (Sr), as an alkaline earth metal, has much wider and richer sources, and it is the 15th most abundant element in the Earth's crust with an estimated abundance of nearly 360 mg/l (Turekian and Wedepohl, 1961). Sr has been widely employed as a dopant for various semiconductors (e.g., TiO_2, zinc oxide and germanium dioxide) to enhance the photocatalytic activities (Yousefi e al. 2015). Moreover, the OH and CO_3 forms of Sr ($Sr(OH)_2$/$SrCO_3$) have been reported to have high photocatalytic activity under visible-light irradiation (Song et al. 2009; Momenian et al., 2013; Márquezherrera et al. 2016).

The aim of this study was to determine the effects of increasing GO/$SrCO_3$ NCs concentrations (1 mg/l, 5 and 10 mg/l), increasing photocatalytic powers (40 W, 80 and 120 W) and increasing sun light irradiation times (60 min, 120 min, 180 and 240 min) on the PCD of four hydrophobic PAHs namely ACL, CRB, BaP and BkF at pH=7.0 and at 22ºC, respectively. The characteristics of the synthesized NPs were assessed using XRD, FESEM, EDX and FTIR analyses, respectively. The acute toxicity assays were operated with Microtox (*Aliivibrio fischeri* or *Vibrio fischeri*) and *Daphnia magna* acute toxicity tests. Cost analysis was evaluated for hydrophobic PAHs removal with GO/$SrCO_3$ NCs by PCD process in PCI ww. ANOVA statistical analysis was used for all experimental samples.

II. MATERIALS AND METHODS

2.1. Material Synthesis

GO was synthesized according to the modified Hummers method (Hummers Jr. and Offeman, 1958). In brief, 3 g of the mixture of GO and Nano-$SrCO_3$ (mass ratio = 2:1) was added to 100 ml of distilled water, and stirred for 0.5 h at 22 ± 1°C. The suspension was then sonicated for 1 h. The resultant composite was recovered by filtration, rinsed with ethanol and then freeze-dried to yield the GO-$SrCO_3$ NCs. Subsequently, dispersing known mass of GO-$SrCO_3$ (30 wt% of the final mass) in a 500 ml of NaOH solution (1 M), and a pre-determined amount of SrCl, (0.5 M) was added dropwise to the dispersion at a rate of 2.0 ml/min using a Titronic Universal titrator (SCHOTT, Mainz, Germany). The resulting material, GO/$SrCO_3$, was then filtered, washed with distilled water until no chloride was detected in the washing water, and then freeze-dried for 48 h. For comparison, a GO/$SrCO_3$ NCs was also prepared by the similar procedure with 20 wt% GO.

2.2. Characterization

2.2.1. X-Ray Diffraction (XRD) Analysis

Powder XRD patterns were recorded on a Shimadzu XRD-7000, Japan diffractometer using Cu Kα radiation (λ=1.5418 Å, 40 kV, 40 mA) at a scanning speed of 1º /min in the 10-80º 2θ range. Raman spectrum was collected with a Horiba Jobin Yvon-Labram HR UV-Visible NIR (200-1600 nm) Raman microscope

spectrometer, using a laser with the wavelength of 512 nm. The spectrum was collected from 10 scans at a resolution of 2 /cm. The zeta potential was measured with a SurPASS Electrokinetic Analyzer (Austria) with a clamping cell at 300 mbar.

2.2.2. Field Emission Scanning Electron Microscopy (FESEM) Analysis

The morphological features and structure of the synthesized catalyst were investigated by a FESEM (FESEM, Hitachi S-4700), equipped with an EDX spectrometry device (TESCAN Co., Model III MIRA) to investigate the composition of the elements present in the synthesized catalyst.

2.2.3. Energy Dispersive X-Ray (EDX) Spectroscopy Analysis

The morphological features and structure of the synthesized catalyst were researhed by an EDX spectrometry device (TESCAN Co., Model III MIRA) to investigate the composition of the elements present in the synthesized catalyst.

2.2.4. Fourier Transform Infrared Spectroscopy (FTIR) Analysis

The FTIR spectra of samples was recorded using the FT-NIR spectroscope (RAYLEIGH, WQF-510).

2.3. Photocatalytic Degradation

Simulated sun light was generated using a 94041A solar simulator (Newport Corporation, Irvine, CA). A cylindrical quartz tank reactor with a Pyrex pillar (80 × 70 mm) was fabricated as the photoreactor. The light intensity reached the reactor was 100 mW/cm^2. The detailed information on the solar simulator and photoreactor has been reported elsewhere (Fu et al., 2017). PAHs were purchased from Alfa Aesar (Ward Hill, MA, USA), and a stock solution of 2 g/l was prepared in methanol. Deionized water (Millipore Co., 18.2 MΩ·cm) was used in preparing all aqueous solutions. Typically, the PCD kinetic tests were conducted under the following conditions: solution volume=250 ml, initial PAHs concentration=1 mg/l, 5 and 10 mg/l, catalyst dosage=50 mg/l, pH=7.0 ± 0.2, and T=22±1ºC. The solution-photocatalyst mixture was first stirred in the dark for 120 min to allow PAHs adsorption to reach equilibrium. Subsequently, photodegradation was initiated by exposing the reactor to the simulated sun light.

2.4. Analytical Methods

UV–Visible spectra of solutions were obtained using an HP 8453 UV–Vis spectrophotometer (Agilent Technologies, Santa Clara, CA, USA). PAHs concentration was determined using an HP 1100 HPLC system (Agilent Technologies, Santa Clara, CA, USA) with a detection limit of 2.5 µg/l at the UV detection wavelength of 250 nm. Photodegradation intermediates were analyzed using an HP7890A/HP5975C gas chromatography-mass spectrometry (GC–MS) system (Agilent Technologies, Santa Clara, CA, USA).

The contributions of various reactive oxygen species (ROS) during the PCD process were investigated by adding scavengers to selectively quench radicals, i.e., potassium peroxymonosulfate (PMS, HSO_5^-), potassium persulfate (PS, $K_2S_2O_8$), and the quenching agent sodium thiosulfate ($Na_2S_2O_3$) were used.

2.4.1. PAHs Measurements

For PAHs and some metabolites (hydroxy-benzoic acid, benzoic acid) analyses the samples were first filtered through a glass fiber filter (47 mm-diameter) to collect the particle-phase in series with a resin column (~10 g XAD-2) and to collect dissolved-phase polybrominated diphenyl ethers. Resin and water filters were ultrasonically extracted for 60 min with a mixture of 1/1 acetone: hexane. All extracts were analyzed for four PAHs gas chromatographically (Agilent 6890N GC) equipped with a mass selective detector (Agilent 5973 inert MSD) (GC-MS). A capillary column (HP5-MS, 30 m, 0.25 mm, 0.25 µm) was used. The initial oven temperature was kept at 50ºC for 1 min, then raised to 200ºC at 25ºC/min and from 200 to 300ºC at 8ºC/min, and then maintained for 5.5 min. High purity He(g) was used as the carrier gas at constant flow mode (1.5 ml/min, 45 cm/s linear velocity). PAHs and their metabolites were identified on the basis of their retention times, target and qualifier ions and were quantified using the internal standard calibration procedure. To determine the degradation intermediates, samples (10 ml each) were collected at 0 min, 60 min, 120 min, 180 min and 240 min. The hydrophobic PAHs (ACL, CRB, BaP and BkF) were performed using a HPLC (Agilent-1100) with a method developed by Lindsey and Tarr (2000). The chromatographic conditions for The hydrophobic PAHs (ACL, CRB, BaP and BkF) determination were as follows: C-18 reverse phase HPLC column (Ace 5C18; 25-cm x 4.6-mm, 5 µm, mobile phase: 50/50 (v/v) methanol/organic-free reagent water). pH, temperature, oxidation-reduction potential (ORP), H_2O_2 were monitored following Standard Methods 2550, 2580, 5220 D and 3550 (Lipps et al., 2022).

2.5. Data Analysis

The pseudo-first-order kinetic model was employed to fit the kinetic data (Zhao et al., 2016; Fu et al., 2017):

$$\ln\left(\frac{C_t}{C_0}\right) = -k \cdot t \quad (1)$$

Where, C_t and C_0 are the PAHs concentrations (µg/l) at the reaction time of t and 0 min, respectively, and k is the rate constant (1/min). The integration of UV–Vis absorbance of PAHs was achieved using the software OriginPro 8 (OriginLab Corporation, Northampton, MA, USA). The correlation fittings between the reaction rate constant and various water quality parameters were conducted by using OriginPro 8 or GraphPad Prism 6 (GraphPad Software, Inc., La Jolla, CA, USA). The fitting models included fourth-order polynomial and sigmoidal (Boltzmann and DoseResp functions) equations.

2.6. Acute Toxicity Assays

2.6.1. Microtox Acute Toxicity Test

Toxicity to the bioluminescent organism *Aliivibrio fischeri (*also called *Vibrio fischeri* or *V. fischeri*) was assayed using the Microtox measuring system according to DIN 38412L34, L341, (EPS 1/ RM/24 1992). Microtox testing was performed according to the standard procedure recommended by the manufacturer (Lange, 1994). A specific strain of the marine bacterium, *V. fischeri*-Microtox LCK 491 kit (Lange, 1994) was used for the Microtox acute toxicity assay. Dr. LANGE LUMIX-mini type luminometer was used for the microtox toxicity assay (Lange, 2010).

2.6.2. *Daphnia magna* Acute Toxicity Test

To test toxicity, 24-h born *Daphnia magna* were used as described in Standard Methods sections 8711A, 8711B, 8711C, 8711D and 8711E, respectively (Lange, 1996). After preparing the test solution, experiments were carried out using 5 or 10 *Daphnia magna* introduced into the test vessels. These vessels had 100 ml of effective volume at 7.0– 8.0 pH, providing a minimum dissolved oxygen (DO) concentration of 6 mg/l at an ambient temperature of 20–25°C. Young *Daphnia magna* were used in the test (≤24 h old); 24–48 h exposure is generally accepted as standard for a *Daphnia magna* acute toxicity test. The results were expressed as mortality percentage of the *Daphnia magna*. Immobile animals were reported as dead *Daphnia magna*.

2.7. Statistical Analysis

ANOVA analysis of variance between experimental data was performed to detect F and *P* values. The ANOVA test was used to test the differences between dependent and independent groups, (Zar, 1984). Comparison between the actual variation of the experimental data averages and standard deviation is expressed in terms of F ratio. F is equal (found variation of the date averages/expected variation of the date averages). *P* reports the significance level, and d.f indicates the number of degrees of freedom. Regression analysis was applied to the experimental data in order to determine the regression coefficient R^2, (Statgraphics Centurion XV, 2005). The aforementioned test was performed using Microsoft Excel Program.

All experiments were carried out three times and the results are given as the means of triplicate samplings. The data relevant to the individual pollutant parameters are given as the mean with standard deviation (SD) values.

III. RESULTS AND DISCUSSION

3.1. Raw Wastewater

Characterization of raw PCI ww taken from the influent of the aeration unit of a PCI ww treatment plant, İzmir, Turkey was performed. The results are given as the mean value of triplicate sampling. The mean values for pH, ORP were recorded as 7.21 and 28.20 mV, respectively. The mean TSS and TVSS concentrations were measured as 310.3 and 250.6 mg/l, respectively. The mean DO, BOD_5, COD_{total}, $COD_{dissolved}$ concentrations were 1.78, 584, 1475 and 1127 mg/l while the Total-N, NH_4-N, NO_3-N, NO_2-N, Total-P, PO_4-P and oil concentrations were measured as 15.40, 2.20, 1.80, 0.05, 10.60, 6.80 and 206 mg/l, respectively. The less hydrophobic ACL and CRB concentrations were 124.2 mg/l and 3.60 mg/l while the more hydrophobic BaP and BkF concentrations were measured as 5.41 and 0.64 mg/l, respectively, in the PCI ww. Physical and chemical properties of the PAHs studied in this work was shown at **Table 1.**

Table 1: Physical and chemical properties of the PAHs studied in this work

PAHs	CAS-No	MF	MW (g/ mol)	T_M (°C)	T_B (°C)	S_W (25°C) (mg/l)	V_P (25°C) (mm Hg)	H (25°C) (atm m^3/mol)	log K_{OA} (25°C)	log K_{OW}	SORC
ACL	208-96-8	$C_{12}H_8$	152	93	280	16.1	6.68E-03	1.14E-04	6.34	3.94	23.56E+10
CRB	86-74-8	$C_{12}H_9N$	167	246	355	1.8	7.50E-07	1.16E-06	8.03	3.72	24.67E+10
BkF	207-08-9	$C_{20}H_{12}$	252	217	480	0.0008	9.70E-10	5.84E-08	11.37	6.11	0.45E+8
BaP	50-32-8	$C_{20}H_{12}$	252	177	495	0.00162	5.49E-09	4.57E-07	11.56	6.13	0.32 E+8

Acenaphthylene (ACL), Carbazole (CRB), Benzo[*k*]fluoranthene (BkF), Benzo[*a*]pyrene (BaP)

MF: Molecular formula, MW: Molecular weight, T_M: Melting point (°C), T_B: Boiling point (°C), S_W: Solubility in water (mg/l), V_P: Vapor pressure (mm Hg), H: Henry's law constant (atm m^3/mol), log K_{OA}: Octanol-air coefficient, log K_{OW}: Octanol-water coefficient, SORC: second-order reaction rate constants (mg/l.s).

3.2. GO/$SrCO_3$ NCs Characteristics

3.2.1. The Results of XRD Analysis

The results of XRD analysis was observed to GO NPs, $SrCO_3$ NPs and GO/$SrCO_3$ NCs, respectively, in PCI ww with PCD process for hydrophobic PAHs removal **(Figure 1).** The characterization peaks were observed at 2θ values of 25.12°, 26.05°, 37.41°, 45.20°, 48.15° and 50.03°, respectively, implying $SrCO_3$ NPs in PCI ww with PCD process for hydrophobic PAHs removal **(Figure 1a)**. The characterization peaks were obtained at 2θ values of 28.33° implying GO NPs in PCI ww with PCD process for hydrophobic PAHs removal **(Figure 1b)**. The characterization peaks were found at 2θ values of 25.17°, 32.30°, 35.18° and 45.57°, respectively, implying GO/$SrCO_3$ NCs in PCI ww with PCD process for hydrophobic PAHs removal **(Figure 1c)**.

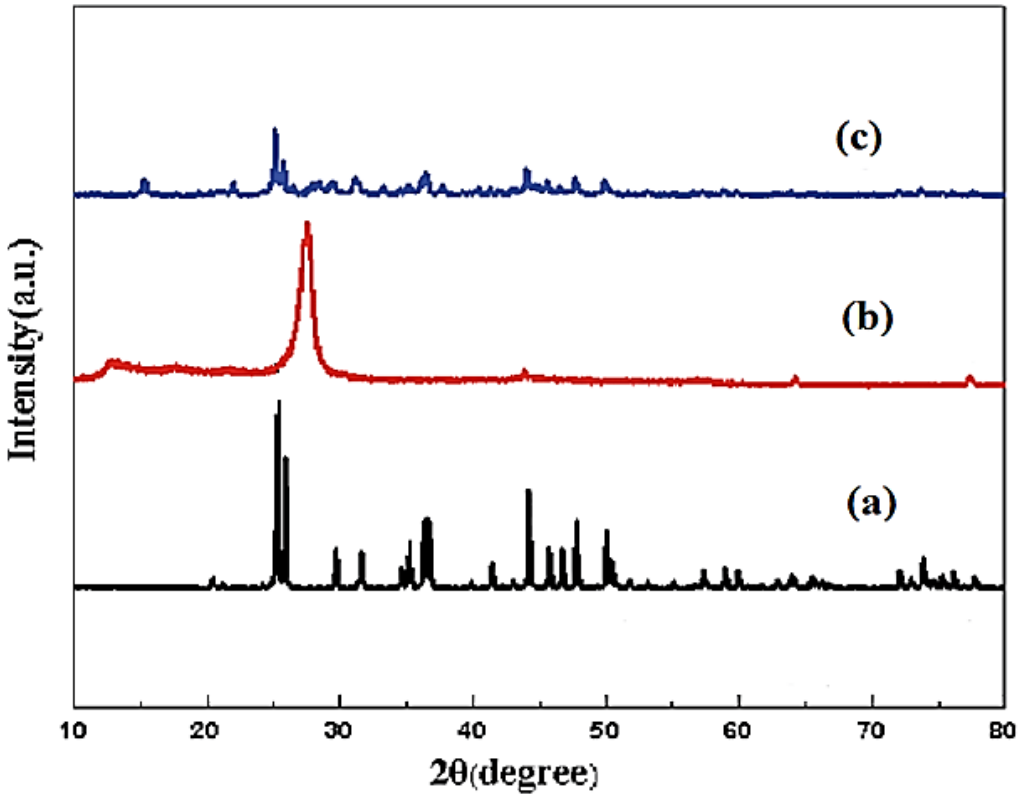

Figure 1: The XRD patterns of **(a)** $SrCO_3$ NPs (black pattern), **(b)** GO NPs (red pattern) and **(c)** GO/$SrCO_3$ (blue pattern) in PCI ww with PCD process for hydrophobic PAHs removal.

3.2.2. The Results of FESEM Analysis

The morphological features of GO NPs (**Figure 2a**), $SrCO_3$ NPs (**Figure 2b**) and GO/$SrCO_3$ NCs (**Figure 2c**), respectively, in PCI ww with PCD process for hydrophobic PAHs removal.

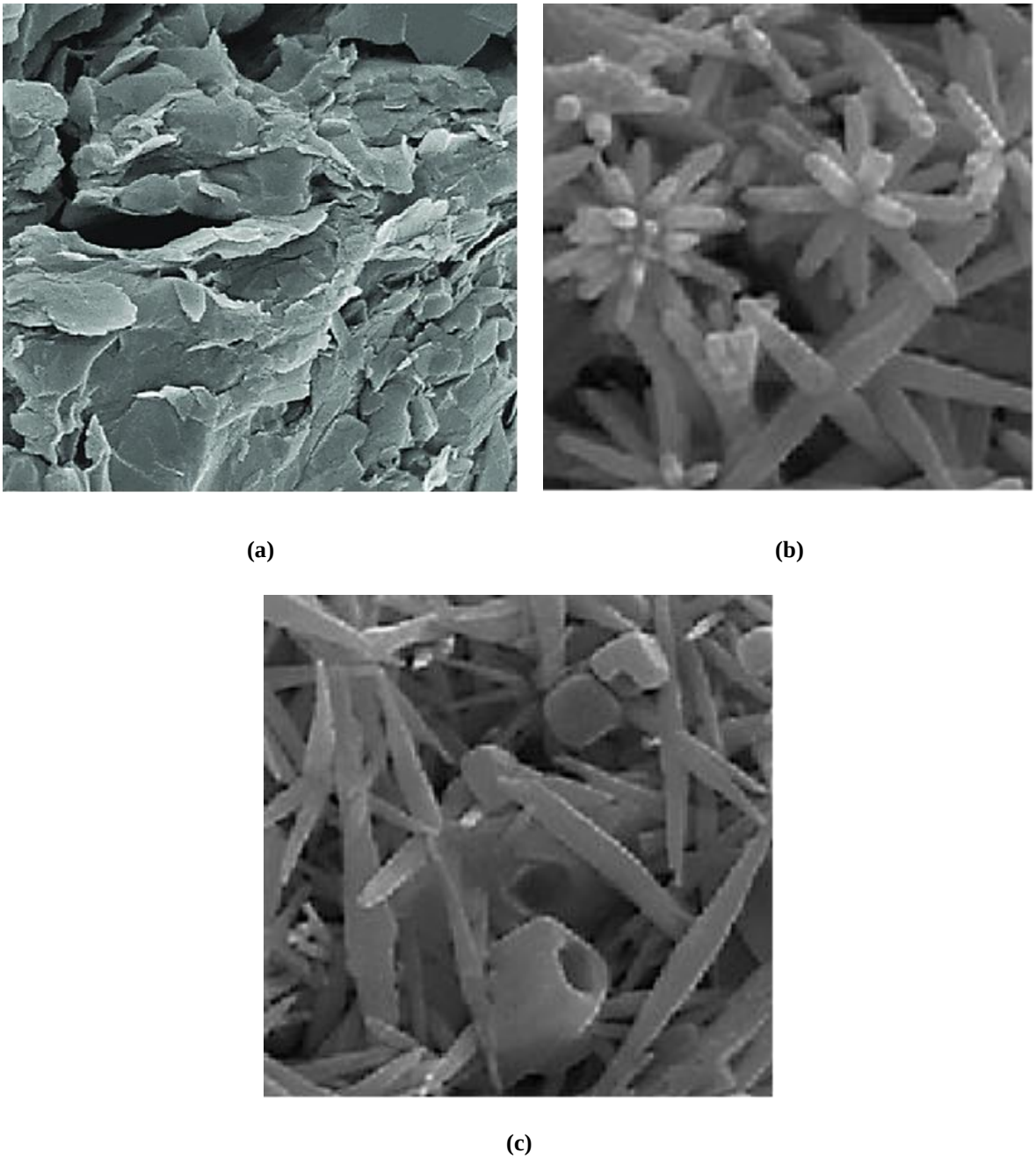

(a) **(b)**

(c)

Figure 2: FESEM images of **(a)** GO NPs, **(b)** $SrCO_3$ NPs and **(c)** GO/$SrCO_3$ NCs in PCI ww with PCD process for hydrophobic PAHs removal (FESEM images size: 200 nm).

3.2.3. The Results of EDX Analysis

The EDX analysis was also performed to investigate the composition of GO NPs (**Figure 3a**), $SrCO_3$ NPs (**Figure 3b**) and GO/$SrCO_3$ NCs (**Figure 3c**), respectively, in PCI ww with PCD process for hydrophobic PAHs removal.

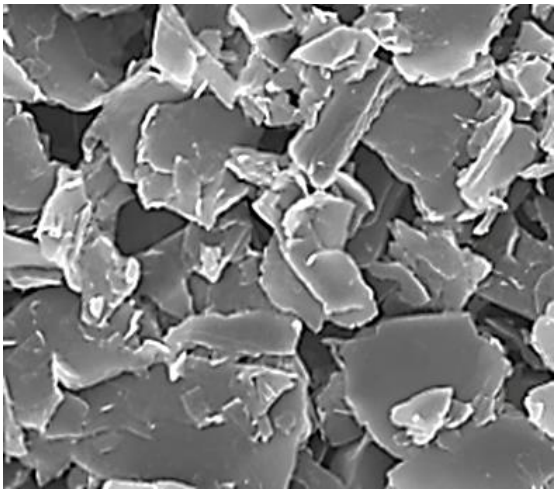

(a)

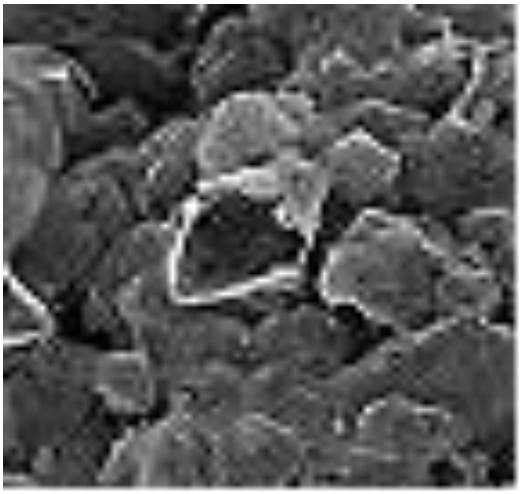

(b)

(c)

Figure 3: EDX spectrum of **(a)** GO NPs, **(b)** $SrCO_3$ NPs and **(c)** GO/$SrCO_3$ NCs, respectively, in PCI ww with PCD process for hydrophobic PAHs removal (EDX spectrum size: 200 nm).

3.2.4. The Results of FTIR Analysis

The FTIR spectrum of SrCO3 NPs (red spectrum), GO NPs (black spectrum) and GO/$SrCO_3$ NCs (blue spectrum), respectively, in PCI ww with PCD process for hydrophobic PAHs removal **(Figure 4)**. The main peaks of FTIR spectrum for $SrCO_3$ NPs was observed at 3430 cm^{-1}, 1771 cm^{-1}, 1450 cm^{-1}, 1065 cm^{-1}, 851 $cm^{-1}$and 695 cm^{-1} wavenumber, respectively (**Figure 4a**). The main peaks of FTIR spectrum for GO NPs was obtained at 3172 cm^{-1}, 1705 cm^{-1}, 1286 cm^{-1} and 803 cm^{-1}, respectively (**Figure 4b**). The main peaks of FTIR spectrum for GO/$SrCO_3$ NCs was determined at 3426 cm^{-1}, 2117 cm^{-1}, 1451 cm^{-1}, 850 cm^{-1}, 817 cm^{-1} and 692 cm^{-1}, respectively (**Figure 4c**).

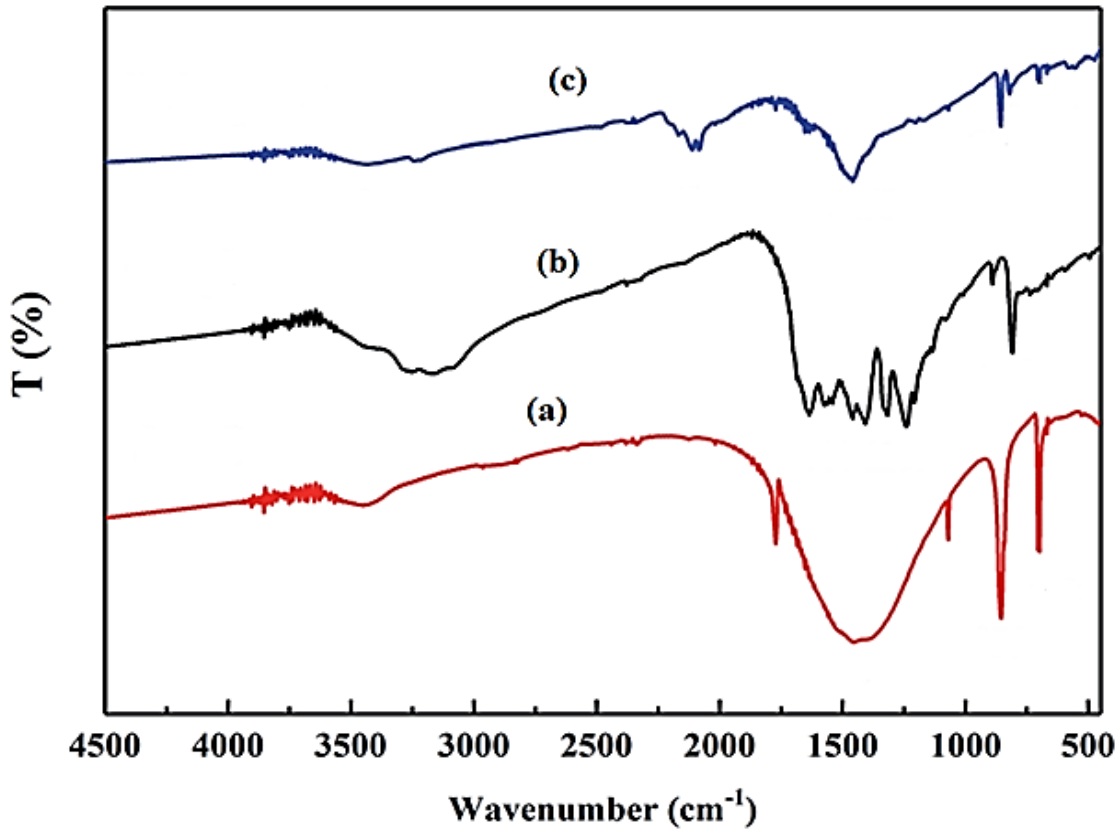

Figure 5: FTIR spectrum of **(a)** $SrCO_3$ NPs (red spectrum), **(b)** GO NPs (black spectrum) and **(c)** GO/$SrCO_3$ NCs (blue spectrum) in PCI ww with PCD process for hydrophobic PAHs removal.

3.3. Effect of increasing sun light irradiation times on PCD of hydrophobic PAHs in PCI ww

The effects of increasing sun light irraditiaon times (60 min, 120 min, 180 and 240 min) were measured in PAHs [less hydrophobic (ACL, CRB) and more hydrophobic (BaP, BkF)] at 100 mW/cm^2, at 120 W, at pH=7.0 at 22^{o}C, respectively (**Table 2**). The maximum 83%ACL, 84%CRB, 87%BaP and 89%BkF hydrophobic PAHs removals were indicated after 240 min sun light irradiation time, at 100 mW/cm^2, at 100 W, at pH=7.0 and at 22^{o}C, respectively (**Table 2**). The increasing sun light irradiaiton times were affected positively effect for the PCD of hydrophobic PAHs (ACL, CRB, BaP and BkF) during sun light irradiation process (**Table 2).**

Table 2: Effect of increasing sun light irradiation times on PCD of hydrophobic PAHs in PCI ww, at 100 mW/cm^2, at pH=7.0 and at 22^{o}C, respectively (n=3, mean values).

Parameter	Hydrophobic PAHs removals (%)			
	Less hydrophobic		More hydrophobic	
	ACL	CRB	BaP	BkF
Sun light irradiation times (min)				
60	58	63	64	68
120	67	71	68	70
180	76	79	75	82
240	83	84	87	89

3.4. Effect of increasing photocatalytic powers on PCD of hydrophobic PAHs in PCI ww

The effects of increasing photocatalytic powers (40 W, 80 W and 120 W) were measured in PAHs [less hydrophobic (ACL, CRB) and more hydrophobic (BaP, BkF)] at 100 mW/cm^2, after 240 min, at pH=7.0 at 22^{o}C, respectively (**Table 3**). The maximum 87%ACL, 90%CRB, 92%BaP and 94%BkF hydrophobic PAHs removals were indicated at 120 W photocatalytic power, at 100 mW/cm^2, after 240 min, at pH=7.0 and at 22^{o}C, respectively

(**Table 3**). The increasing photocatalytic powers were affected positively effect for the PCD of hydrophobic PAHs (ACL, CRB, BaP and BkF) during sun light irradiation process (**Table 3).**

Table 3: Effect of increasing photocatalytic power on PCD of hydrophobic PAHs in PCI ww, at 100 mW/cm^2, at pH=7.0 and at 22^{o}C, respectively (n=3, mean values).

Parameters	Hydrophobic PAHs removals (%)			
	Less hydrophobic		More hydrophobic	
	ACL	CRB	BaP	BkF
Photocatalytic Powers (W)				
40	59	65	71	73
80	72	74	81	78
120	87	90	92	94

3.5. Effect of increasing GO/$SrCO_3$ NCs concentrations on PCD of hydrophobic PAHs in PCI ww

Based on the preliminary studies the optimum removals of some less hydrophobic (ACL, CRB) and more hydrophobic (BaP, BkF)] PAHs were researched at 100 mW/cm^2, at 120 W, after 240 min, at pH=7.0 and at 22^{o}C, respectively (**Table 4**). The maximum 98%ACL, 98%CRB, 98%BaP and 99%BkF hydrophobic PAHs removals were found at 10 mg/l GO/$SrCO_3$ NCs concentration at 100 mW/cm^2, at 120 W, after 240 min, at a pHof 7.0 and at 22^{o}C, respectively (**Table 4**). The increasing GO/$SrCO_3$ NCs concentrations were found to be positively affect for the PCD of hydrophobic PAHs (ACL, CRB, BaP and BkF) during sun light irradiation process (**Table 4).**

Table 4: Effect of increasing GO/$SrCO_3$ NCs on PCD of hydrophobic PAHs in PCI ww, at 100 mW/cm^2, at pH=7.0 and at 22^{o}C, respectively (n=3, mean values).

Parameters	Hydrophobic PAHs removals (%)			
	Less hydrophobic		More hydrophobic	
	ACL	CRB	BaP	BkF
GO/$SrCO_3$ NCs concentrations (mg/l)				
1	79	77	83	95
5	91	88	89	97
10	98	98	98	99

An optimum GO/$SrCO_3$ NCs concentration of 10 mg/l increase the ionic strength of the aqueous phase, driving the PAHs to the bulk–bubble interface in a photocatalytic reactor. This, increases the partitioning of the PAH species upon radical scavengers in a photocatalytic reactor. Beyond the partitioning enhancement, the presence of salt reduces the vapor pressure and increases the surface tension of the PAHs (Chakinala et al., 2008). Therefore, the solubility of the solution decreases and the diffusion of solutes decreases from the bulk solution to the bubble–liquid interface with administration of decreasing GO/$SrCO_3$ NCs concentrations in the photocatalytic reactor (Fu e al., 2018). The high PAH removals in raised GO/$SrCO_3$ NCs concentrations can be explained by the fact that a higher amount of GO/$SrCO_3$ NCs will create more salting out effect than the lower amount and thus increase the interfacial concentration of the PAHs. In our study, no contribution of GO/$SrCO_3$ NCs > 10 mg/l to the PAH yields could be attributed to the sinergistic and antagonistic effects of the by-products and to the more hydrophobic (BaP, BkF) and less hydropholic (ACL, CRB) nature of PAHs present in PCI ww **(Table 4).**

3.6. Acute Toxicity Assays

3.6.1. Effect of Increasing GO/$SrCO_3$ NCs Concentrations on the Microtox Acute Toxicity Removal Efficiencies in PCI ww at Increasing PCD Time and Temperature

In Microtox with *Aliivibrio fischeri* (or *Vibrio fischeri*) acute toxicity test, the initial EC_{90} values at pH=7.0 was found as 825 mg/l at 25^{o}C (**Table 5: SET 1**). After 60 min, 120 and 180 min PCD time, the EC_{90} values decreased to EC_{57}=414 mg/l to EC_{22}=236 mg/l and to EC_{12}=165 mg/l in GO/$SrCO_3$ NCs=10 mg/l at 30^{o}C (**Table 5: SET 3**). The Microtox acute toxicity removals were 40.89%, 79.78% and 90.91% after 60 min, 120 min and 180 min, respectively, in GO/$SrCO_3$ NCs=10 mg/l and at 30^{o}C (**Table 5: SET 3**).

Table 5: Effect of increasing $GO/SrCO_3$ NCs concentrations on Microtox acute toxicity in PCI ww after PCD process, at 30ºC and at 60ºC, respectively.

No	Parameters	Microtox Acute Toxicity Values, * EC (mg/l)							
		25ºC							
		0. min		60. min		120. min		180. min	
		*EC_{90}		*EC		*EC		*EC	
1	Raw ww, control	825		EC_{70}=510		EC_{60}=650		EC_{49}=638	
		30ºC				60ºC			
		0. min	60. min	120. min	180. min	0. min	60. min	120. min	180. min
		*EC_{90}	*EC	*EC	*EC	*EC_{90}	*EC	*EC	*EC
2	Raw ww, control	825	EC_{70}= 580	EC_{50}= 580	EC_{39}= 548	825	EC_{55}= 550	EC_{40}= 590	EC_{29}= 688
3	$GO/SrCO_3$ NCs=1 mg/l	825	EC_{62}= 422	EC_{27}= 241	EC_{17}= 168	825	EC_{57}= 419	EC_{22}= 266	EC_{12}= 150
	$GO/SrCO_3$ NCs=5 mg/l	825	EC_{62}= 421	EC_{27}= 239	EC_{17}= 167	825	EC_{57}= 414	EC_{22}= 232	EC_{12}= 161
	$GO/SrCO_3$ NCs=10 mg/l	825	EC_{57} =414	EC_{22}= 236	EC_{12}= 165	825	EC_{52}= 550	EC_{17}= 540	EC_7= 500
* EC values were calculated based on COD_{dis} (mg/l).									

The EC_{90} values decreased to EC_{51}, to EC_{16} and to EC_6 after 60 min, 120 and 180 min, respectively, in $GO/SrCO_3$ NCs=10 mg/l, at 60ºC (**Table 5: SET 3**). The EC_{52}, the EC_{17} and the EC_7 values were measured as 550 mg/l, 540 and 500 mg/l, respectively, in $GO/SrCO_3$ NCs=10 mg/l at 60ºC. The toxicity removal efficiencies were 46.44%, 85.34% and 96.47% after 60 min, 120 and 180 min, respectively, in $GO/SrCO_3$ NCs=10 mg/l, at 60ºC (**Table 5: SET 3**). 96.47% maximum Microtox acute toxicity removals was found in $GO/SrCO_3$ NCs=10 mg/l after 180 min and at 60ºC (**Table 5: SET 3**).

The EC_{90} values decreased to EC_{62}=422 mg/l to EC_{27}=241 mg/l and to EC_{17}=168 mg/l after 60 min, 120 and 180 min, respectively, in $GO/SrCO_3$ NCs=1 mg/l at 30ºC (**Table 5: SET 3**). The EC_{90} values decreased to EC_{62}=421 mg/l to EC_{27}=239 mg/l and to EC_{17}=167 mg/l after 60 min, 120 and 180 min, respectively, in $GO/SrCO_3$ NCs=5 mg/l at 30ºC. The Microtox acute toxicity removals were 85.34% and 86.42% in 1 mg/l and 5 mg/l $GO/SrCO_3$ NCs, respectively, after 180 min, at 30ºC (**Table 5: SET 3**).

The EC_{90} values decreased to EC_{57}=419 mg/l to EC_{22}=266 mg/l and to EC_{12}=150 mg/l after 60 min, 120 and 180 min, respectively, in $GO/SrCO_3$ NCs=1 mg/l at 60ºC (**Table 5: SET 3**). The EC_{90} values decreased to EC_{57}=414 mg/l to EC_{22}=232 mg/l and to EC_{12}=161 mg/l after 60 min, 120 and 180 min, respectively, in $GO/SrCO_3$ NCs=5 mg/l at 60ºC. The Microtox acute toxicity removals were 90.89% and 91.82% in 1 mg/l amd 5 mg/l $GO/SrCO_3$ NCs, respectively, after 180 min, at 60ºC (**Table 5: SET 3**).

3.6.2. Effect of Increasing $GO/SrCO_3$ NCs Concentrations on the *Daphnia magna* Acute Toxicity Removal Efficiencies in PCI ww at Increasing PCD Time and Temperature

The initial EC_{50} values were observed as 850 mg/l at 25ºC (**Table 6: SET 1**). After 60 min, 120 and 180 min time, the EC_{50} values decreased to EC_{31}=350 mg/l to EC_{17}=240 mg/l and to EC_{12}=90 mg/l in $GO/SrCO_3$ NCs=10 mg/l, at 30ºC (**Table 6: SET 3**). The toxicity removal efficiencies were 41.88%, 71.79% and 81.57% after 60 min, 120 min and 180 min, respectively, in DOX=30 mg/l at 30ºC (**Table 6: SET 3**).

Table 6: Effect of increasing $GO/SrCO_3$ NCs concentrations on *Daphnia magna* acute toxicity in PCI ww after PCD process, at 30ºC and at 60ºC.

No	Parameters	*Daphnia magna* Acute Toxicity Values, * EC (mg/l)			
		25ºC			
		0. min	60. min	120. min	180. min
		*EC_{50}	*EC	*EC	*EC
1	Raw ww, control	850	EC_{45}=625	EC_{40}=370	EC_{29}=153

		30ºC				60ºC			
		0. min	**60. min**	**120. min**	**180. min**	**0. min**	**60. min**	**120. min**	**180. min**
		***EC_{50}**	***EC**	***EC**	***EC**	***EC_{50}**	***EC**	***EC**	***EC**
2	Raw ww, control	850	EC_{39}= 468	EC_{34}= 228	EC_{23}= 111	850	EC_{34}= 373	EC_{29}= 210	EC_{18}= 71
3	$GO/SrCO_3$ NCs=1 mg/l	850	EC_{32}= 450	EC_{22}= 145	EC_{17}= 260	850	EC_{32}= 130	EC_{17}= 425	EC_{12}= 340
	$GO/SrCO_3$ NCs=5 mg/l	850	EC_{37}= 450	EC_{22}= 175	EC_{17}= 100	850	EC_{32}= 425	EC_{17}= 140	EC_7= 90
	$GO/SrCO_3$ NCs=10 mg/l	850	EC_{32}= 350	EC_{17}= 240	EC_{12}= 90	850	EC_{27}= 150	EC_{12}= 60	EC7= 375
* EC values were calculated based on COD_{dis} (mg/l).									

The EC_{50} values decreased to EC_{26} to EC_{11} and to EC_6 after 60 min, 120 and 180 min, respectively, in $GO/SrCO_3$ NCs=10 mg/l at 60ºC (**Table 6: SET 3**). The EC_{27}, the EC_{12} and the EC_7 values were measured as 150 mg/l, 60 mg/l and 375 mg/l, respectively, in $GO/SrCO_3$ NCs=10 mg/l at 60ºC. The toxicity removals were 52.97%, 82.65% and 92.38% after 60 min, 120 and 180 min, respectively, in $GO/SrCO_3$ NCs=10 mg/l at 60ºC (**Table 6: SET 3**). 92.38% maximum *Daphnia magna* acute toxicity removal was obtained in $GO/SrCO_3$ NCs=10 mg/l after 180 min and at 60ºC (**Table 6: SET 3**).

The EC_{50} values decreased to EC_{37}=450 mg/l to EC_{22}=145 mg/l and to EC_{17}=260 mg/l after 60 min, 120 and 180 min, respectively, in $GO/SrCO_3$ NCs=1 mg/l at 30ºC (**Table 6: SET 3**). The EC_{50} values decreased to EC_{37}=450 mg/l to EC_{22}=175 mg/l and to EC_{17}=100 mg/l after 60 min, 120 and 180 min, respectively, in $GO/SrCO_3$ NCs=5 mg/l and at 30ºC. The *Daphnia magna* acute toxicity removals were 72.25% and 73.59% in 1 mg/l and 5 mg/l $GO/SrCO_3$, respectively, after 180 min and at 30ºC (**Table 6: SET 3**).

The EC_{50} values decreased to EC_{32}=130 mg/l to EC_{17}=425 mg/l and to EC_{12}=340 mg/l after 60 min, 120 and 180 min, respectively, in $GO/SrCO_3$ NCs=1 mg/l and at 60ºC (**Table 6: SET 3**). The EC_{50} values decreased to EC_{32}=425 mg/l to EC_{17}=140 mg/l and to EC_7=90 mg/l after 60 min, 120 and 180 min, respectively, in $GO/SrCO_3$ NCs=5 mg/l and at 60ºC. The *Daphnia magna* acute toxicity removals were 83.08% and 91.69% in 1 mg/l and 5 mg/l $GO/SrCO_3$ NCs, respectively, after 180 min and at 60ºC (**Table 6: SET 3**).

Increasing the $GO/SrCO_3$ NCs concentrations from 1 mg/l to 5 mg/l did not have a positive effect on the decrease of EC_{50} values as shown in **Table 6 at SET 3**. $GO/SrCO_3$ NCs concentrations > 10 mg/l decreased the acute toxicity removals by hindering the PCD process. Similarly, a significant contribution of increasing $GO/SrCO_3$ NCs concentration to acute toxicity removal at 60ºC after 180 min of PCD time was not observed. Low toxicity removals found at high $GO/SrCO_3$ NCs concentrations could be attributed to their detrimental effect on the *Daphnia magna* (**Table 6: SET 3**).

3.6.3. Direct Effects of $GO/SrCO_3$ NCs Concentrations on the Acute Toxicity of Microtox and *Daphnia magna* without PCI ww after PCD Process

The acute toxicity test was performed in the samples containing 1 mg/l, 5 and 10 mg/l $GO/SrCO_3$ NCs concentrations, at 25ºC. In order to detect the direct responses of Microtox and *Daphnia magna* to the increasing $GO/SrCO_3$ NCs concentrations the toxicity test were performed without PCI ww after PCD process, at 25ºC. The initial EC values and the the EC_{50} values were measured in the samples containing increasing $GO/SrCO_3$ NCs concentrations after 180 min PCD time. **Table 7** showed the responses of Microtox and *Daphnia magna* to increasing $GO/SrCO_3$ NCs concentrations.

Table 7: The responses of Microtox and *Daphnia magna* acute toxicity tests in addition of increasing $GO/SrCO_3$ NCs concentrations without PCI ww during PCD process after 180 min PCD time, at 25ºC.

$GO/SrCO_3$ NCs Conc. (mg/l)	**Microtox Acute Toxicity Test**			***Daphnia magna* Acute Toxicity Test**		
	Initial EC_{50} Value (mg/l)	**Inhibitions after 180 min**	**EC Values (mg/l)**	**Initial EC_{50} Value (mg/l)**	**Inhibitions after 180 min**	**EC Values (mg/l)**
1	EC_{10}= 21	-	-	EC_{10}= 36	-	-
5	EC_{15}= 76	3	EC_2= 2	EC_{20}= 96	5	EC_3= 4
10	EC_{20}= 146	5	EC_4= 5	EC_{30}= 196	6	EC_6= 10

The acute toxicity originating only from 1 mg/l, 5 mg/l and 10 mg/l GO/$SrCO_3$ NCs were found to be low (**Table 7**). 1 mg/l GO/$SrCO_3$ NCs did not exhibited toxicity to *Aliivibrio fischeri* (or *Vibrio fischeri*) and *Daphnia magna* before and after 180 min PCD time. The toxicity atributed to the 5 mg/l, 30 mg/l and 10 mg/l GO/$SrCO_3$ NCs were found to be low in the samples without PCI ww after PCD process for the test organisms mentioned above. The acute toxicity originated from the GO/$SrCO_3$ NCs decreased significantly to EC_2 and EC_4 after 180 min PCD time. Therefore, it can be concluded that the toxicity originating from the GO/$SrCO_3$ NCs is not significant and the real acute toxicity throughout PCD process was attributed to the PCI ww, to their metabolites and to the PCD by-products (**Table 7**).

IV. CONCLUSIONS

The results of this study showed that the hydrophobic PAHs in a PCI ww with high benzene rings could be removed as successfully as the less hydrophobic PAHs (ACL and CRB) and more hydrophobic PAHs (BaP and BkF) with PCD under sun light irradiation process.

The maximum 83%ACL, 84%CRB, 87%BaP and 89%BkF hydrophobic PAHs removals were indicated after 240 min sun light irradiation time, at 100 mW/cm^2, at 100 W, at pH=7.0 and at 22ºC, respectively.

The maximum 87%ACL, 90%CRB, 92%BaP and 94%BkF hydrophobic PAHs removals were indicated at 120 W photocatalytic power, at 100 mW/cm^2, after 240 min, at pH=7.0 and at 22ºC, respectively.

The maximum 98%ACL, 98%CRB, 98%BaP and 99%BkF hydrophobic PAHs removals were found at 10 mg/l GO/$SrCO_3$ NCs concentration at 100 mW/cm^2, at 120 W, after 240 min, at a pHof 7.0 and at 22ºC, respectively.

96.47% maximum Microtox acute toxicity removals was found in GO/$SrCO_3$ NCs=10 mg/l after 180 min and at 60ºC. 92.38% maximum *Daphnia magna* acute toxicity removal was obtained in GO/$SrCO_3$ NCs=10 mg/l after 180 min and at 60ºC. Increasing the GO/$SrCO_3$ NCs concentrations from 1 mg/l to 5 mg/l did not have a positive effect on the decrease of EC_{50} values. GO/$SrCO_3$ NCs concentrations > 10 mg/l decreased the acute toxicity removals by hindering the PCD process. Similarly, a significant contribution of increasing GO/$SrCO_3$ NCs concentration to acute toxicity removal at 60ºC after 180 min of PCD time was not observed.

In sum, GO/$SrCO_3$ NCs holds the potential to serve as a highly effective and robust photocatalyst for energy-effective photodegradation of PAHs (and potentially other persistent organic pollutants) in complex water matrices, and the multiplicative model is a useful tool for predicting the photocatalytic performances under several experimental conditions.

Acknowledgement

This research study was undertaken in the Environmental Microbiology Laboratories at Dokuz Eylül University Engineering Faculty Environmental Engineering Department, Izmir, Turkey. The authors would like to thank this body for providing financial support.

REFERENCES

[1]. Banjoo, D.R. and Nelson, P.K. Improved ultrasonic extraction procedure for the determination of polycyclic aromatic hydrocarbons in sediments, Journal of Chromatography A, 1066 (2005) 9-18.
[2]. Chakinala, A.G., Gogate, P.R., Chand, R., Bremner, D.H., Molina, R. and Burgess, A.E. Intensification of oxidation capacity using chloroalkanes as additives in hydrodynamic and acoustic cavitation reactors, Ultrasonics Sonochemistry, 15 (2008) 164–170.
[3]. Fu, J., Sheng, S., Wen, T., Zhang, Z.-M., Wang, Q., Hu, Q.-X., Li, Q.-S., An, S.-Q. and Zhu, H.- L. Polycyclic aromatic hydrocarbons in surface sediments of the Jialu River, Ecotoxicology 20 (2011a) 940–950
[4]. Fu, J., Ding, Y.-H., Li, L., Sheng, S., Wen, T., Yu, L.-J., Chen, W., An, S.-Q. and Zhu, H.-L. Polycyclic aromatic hydrocarbons and ecotoxicological characterization of sediments from the Huaihe River, China, Journal of Environmental Monitoring and Assessment, 13 (2011b) 597–604.
[5]. Fu, J., Gong, Y., Zhao, X., O'Reilly, S.E. and Zhao, D. Effects of oil and dispersant on formation of marine oil snow and transport of oil hydrocarbons, Environmental Science & Technology, 48 (2014) 14392–14399.
[6]. Fu, J., Gong, Y., Cai, Z., O'Reilly, S.E. and Zhao, D. Mechanistic investigation into sunlight-facilitated photodegradation of pyrene in seawater with oil dispersants, Marine Pollution Bulletin, 114 (2017) 751–758.
[7]. Fu, J., Kyzasc, G.Z., Cai, Z., Deliyanni, E.A., Liu, W. and Zhao, D. Photocatalytic degradation of phenanthrene by graphite oxide-TiO2-Sr (OH)2/SrCO3 nanocomposite under solar irradiation: Effects of water quality parameters and predictive modeling, Chemical Engineering Journal, 335 (2018) 290–300.
[8]. Gong, Y., Fu, J., O'Reilly, S.E. and Zhao, D. Effects of oil dispersants on photodegradation of pyrene in marine water, Journal of Hazardous Materials, 287 (2015) 142–150.
[9]. Guo, J., Zhu, S., Chen, Z., Li, Y., Yu, Z., Liu, Q., Li, J., Feng, C. and Zhang, D. Sonochemical synthesis of TiO2 nanoparticles on graphene for use as photocatalyst, Ultrasonics Sonochemistry, 18 (2011) 1082–1090.
[10]. Hummers Jr., W.S. and Offeman, R.E. Preparation of graphitic oxide, Journal of the American Chemical Society, 80 (1958) 1339.
[11]. Lange, B. LUMISmini, Operating Manual. Dusseldorf, Germany: Dr Bruno LANGE., 1994.
[12]. Lange, B. LUMIXmini type luminometer. Dusseldorf: Dr LANGE Company., 1996.
[13]. Lange, B. Vibrio fischeri -Microtox LCK 491 kit. Germany: Dr LANGE., 2010.
[14]. Liang, Y., Li, Y., Wang, H., Zhou, J., Wang, J., Regier, T. and Dai, H. Co3O4 nanocrystals on graphene as a synergistic catalyst for oxygen reduction reaction, Nature Materials, 10 (2011) 780–786.
[15]. Lindsey, M.E. and Tarr, M.A. Quantitation of hydroxyl radical during Fenton oxidation following a single addition of iron and peroxide, Chemosphere 41 (2000) 409-417.

[16]. Lipps, W.C., Braun-Howland, E.B., Baxter, T.E. (2022). Standard Methods for the Examination of Water and Wastewater. (24th. Edition). Lipps, W.C., Braun-Howland, E.B., Baxter, T.E. (editors), American Public Health Association (APHA), American Water Works Association (AWWA), Water Environment Federation (WEF), Elevate Your Standards. American Public Health Association 800 I Street, NW Washington DC: 20001-3770, USA, December 1, 2022; ISBN:9780875532998.
[17]. Márquezherrera, A., Ovandomedina, V., Castilloreyes, B., Zapatatorres, M., Meléndezlira, M. and Gonzálezcastañeda, J. Facile synthesis of SrCO3-Sr(OH)2/PPy nanocomposite with enhanced photocatalytic activity under visible light, Materials, 9 (2016) 30.
[18]. Momenian, H.R., Gholamrezaei, S., Salavati-Niasari, M., Pedram, B., Mozaffar, F. and Ghanbari, D. Sonochemical synthesis and photocatalytic properties of metal hydroxide and carbonate (M: Mg, Ca, Sr or Ba) nanoparticles, Journal of Cluster Science, 24 (2013) 1031–1042.
[19]. Qu, L., Liu, Y., Baek, J.B. and Dai, L. Nitrogen-doped graphene as efficient metal-free electrocatalyst for oxygen reduction in fuel cells, ACS Nano, 4 (2010) 1321–1326.
[20]. Quesada-Peñate, I., Julcour-Lebigue, C., Jáuregui-Haza, U.-J., Wilhelm, A-M. and Darie, D.H. Sonolysis of levodopa and paracetamol in aqueous solutions, Ultrasonics Sonochemistry, 16 (2009) 610-616.
[21]. Song, L., Zhang, S. and Chen, B. A novel visible-light-sensitive strontium carbonate photocatalyst with high photocatalytic activity, Catalysis Communications, 10 (2009) 1565–1568.
[22]. Sponza, D.T. and Oztekin, R. Effect of sonication assisted by titanium dioxide and ferrous ions on Poly aromatic hydrocarbons (PAHs) and toxicity removals from a petrochemical industry wastewater in Turkey, Journal of Chemical Technology and Biotechnology, 85 (2010) 913–925
[23]. Statgraphics Centurion XV, sofware, StatPoint Inc, Statgraphics Centurion XV, Herndon, VA, USA, 2005.
[24]. Stengl, V., Henych, J., Vomáčka, P. and Slušná, M. Doping of TiO2-GO and TiO2-rGO with noble metals: synthesis, characterization and photocatalytic performance for azo dye discoloration, Photochemistry and Photobiology, 89 (2013) 1038–1046.
[25]. Turekian, K.K. and Wedepohl, K.H. Distribution of the elements in some major units of the Earth's crust, Geological Society of America bulletin, 72 (1961) 175.
[26]. Yousefi, R., Jamali-Sheini, F., Cheraghizade, M., Khosravi-Gandomani, S., Sáaedi, A., Huang, N.M., Wan, J.B. and Azarang, M. Enhanced visible-light photocatalytic activity of strontium-doped zinc oxide nanoparticles, Materials Science in Semiconductor Processing, 32 (2015) 152.
[27]. Zar, J.H. Biostatistical analysis, Prentice-Hall, Englewood Cliffs, 1984.
[28]. Zeng, P., Zhang, Q., Zhang, X. and Peng, T. Graphite oxide–TiO2 nanocomposite and its efficient visible-light-driven photocatalytic hydrogen production, Journal of Alloys and Compounds, 516 (2012) 85–90.
[29]. Zhao, K., Zhao, S.L., Qi, J., Yin, H.J., Gao, C., Khattak, A.M., Wu, Y.J., Iqbal, A., Wu, L., Gao, Y., Yu, R.B. and Tang, Z.Y. Cu2O clusters grown on TiO2 nanoplates as efficient photocatalysts for hydrogen generation, Inorganic Chemistry Frontiers, 3 (2016) 488–493.

Rukiye Öztekin, et. al. "Treatment of Hydrophobic Polyaromatic Hydrocarbons (PAHs) using Graphene oxide/Strontium carbonate (GO/SrCO3) Nanocomposite via Photocatalytic Degradation and the Evaluation of Experimental Results with Microtox and Daphnia magna Acute Toxicity Assays." *International Journal of Engineering and Science*, vol. 13, no. 6, 2023, pp. 01-13.